Available online at www.sciencedirect.com
ScienceDirect
Journal of the European Ceramic Society 31 (2011) 2459–2462
www.elsevier.com/locate/jeurceramsoc

Crystallization and magnetic property of iron oxide nanoparticles precipitated in silica glass matrix

Y. Masubuchi *, Y. Sato, A. Sawada, T. Motohashi, H. Kiyono, S. Kikkawa

Faculty of Engineering, Hokkaido University, N13-W8, Kita-ku, Sapporo 060-8628, Japan

Available online 8 March 2011

Abstract

Crystallization and magnetic property of Fe_2O_3 nanoparticle precipitated in SiO_2 matrix was investigated. Fe_2O_3/SiO_2 nanocomposite thin film was obtained by annealing of the amorphous Fe–Si–O thin film deposited by RF-magnetron sputtering of $(\alpha\text{-}Fe_2O_3)_{1-x}/(SiO_2)_x$ composite targets. The Fe_2O_3 crystallite size increased with decreasing SiO_2 area ratio, x of the target and increasing annealing temperature. ε-Fe_2O_3 with the crystallite size of 20–30 nm was obtained after annealing the film deposited in SiO_2 area ratio, $x = 0.33$–0.42 at 900 °C. Lower SiO_2 area ratio (x) than 0.25 and higher annealing temperature resulted in precipitation of α-Fe_2O_3 with the larger crystallite size than 40 nm. In the case of SiO_2 area ratio, $x \geq 0.50$, the annealed film was amorphous and showed higher magnetization and smaller coercivity due to the precipitation of very small crystalline γ-Fe_2O_3. The ε-Fe_2O_3/SiO_2 composite thin film showed ferromagnetic hysteresis with coercive force of 0.14 T.

Keywords: Iron oxide; Films; Nanocomposites; Magnetic properties; Thermal annealing

1. Introduction

Iron (III) oxide (Fe_2O_3) has four polymorphs: α-, β-, γ- and ε-Fe_2O_3.[1] The α- and γ-Fe_2O_3 have been extensively studied for applications in non-toxic inorganic red pigment and magnetic recording media, respectively. α-Phase has a corundum structure and exhibits antiferromagnetic characteristic ($T_N = 950$ K) with slightly canting in spins resulting in a weak ferromagnetism.[2,3] γ-Phase has a spinel structure and ferrimagnetic behavior with a Curie temperature (T_C) of 928 K.[1,4] Recently, enormously large room temperature coercivity about 2 T was reported on ε-Fe_2O_3 phase,[5–7] but the value is not reproducible.[8,9] It has an orthorhombic structure and is ferromagnetic with $T_C = 480$ K.[6,10] β-Phase is another new phase having a bixbyite structure and exhibits antiferromagnetic feature with a Neel temperature (T_N) of 119 K.[11–13] α-Fe_2O_3 is the thermodynamically most stable among these four polymorphs. Other Fe_2O_3 polymorphs also appear in stabilizing by the surface energy of their particles in nanometer scale. ε-Fe_2O_3 is a phase reported only as nanocomposites with SiO_2 derived by polymerization of TEOS or triethoxysilane.[14,15] In this view point, Gich et al. have reported that the confinement of particle size in the SiO_2 matrix plays an important role in the formation and stabilization of ε-Fe_2O_3 and crystal structure change in the order of $\gamma \rightarrow \varepsilon \rightarrow \alpha$-$Fe_2O_3$ as increase in the nanoparticle size.[16] Recently, the phase transformation among the four Fe_2O_3 polymorphs has been proposed to be $\gamma \rightarrow \varepsilon \rightarrow \beta \rightarrow \alpha$-$Fe_2O_3$ with increasing particle size using the impregnation method.[17] The ε-Fe_2O_3 particle size was in a range of 10–30 nm diameter in those reports.

These ε-Fe_2O_3/SiO_2 nanocomposites have been synthesized by controlling Fe_2O_3 particle size dispersed in SiO_2 matrix in various kinds of chemical route. Aqueous solution of $Fe(NO_3)_2$ was hydrolyzed together with TEOS or triethoxysilane to be confined in silica gel.[6,10] Hydrolysis was also applied on Fe(III) complex with complicated ligands containing –Si(OCH_3) bonds.[8] The droplet size of Fe solution was tried to control in several studies using reverse-micelle or impregnation into mesoporous SiO_2 particels.[5,9,17] It is obviously not easy to control the nanoparticle size in the sol–gel related routes because iron oxide easily precipitates outside SiO_2 matrix to aggregates in a large grain size to form the most stable α-Fe_2O_3 after their thermal treatment. This is the reason why the ε-Fe_2O_3/SiO_2 composites contaminated with α-Fe_2O_3 impurity in most studies. Nano-sized magnetic alloy has been synthesized by simple thermal annealing of an appropriate amorphous film.[18–20] Its

* Corresponding author. Tel.: +81 011 706 6742; fax: +81 011 706 6740.
E-mail address: yuji-mas@eng.hokudai.ac.jp (Y. Masubuchi).

0955-2219/$ – see front matter © 2011 Elsevier Ltd. All rights reserved.
doi:10.1016/j.jeurceramsoc.2011.02.016

nanoparticles precipitate from the amorphous alloy matrix via thermal diffusion during the annealing. The particle size can be controlled in the precipitation only by changing the thermal annealing condition and the starting composition.

In this study, amorphous Fe–Si–O thin films deposited on a silica glass substrate by RF-magnetron sputtering were thermal annealed to precipitate ε-Fe_2O_3 nanoparticles in SiO_2 matrix. The annealed thin films were investigated in their structure and magnetic property.

2. Experimental procedure

Silica glass chips (wedge shape with radius of 38 mm and inner angle of 30°) (99.99%, Kojyundo Chemical Laboratory Co.) were distributed on an α-Fe_2O_3 target (diameter of 76.2 mm) (99.9%, Kojyundo Chemical Laboratory Co.) in the composite targets. Their SiO_2 area ratio was varied from $x = 0.25$ to 0.5 in $(\alpha\text{-}Fe_2O_3)_{1-x}(SiO_2)_x$ by changing the number of the chips. RF-magnetron sputter equipment (JEOL, JEC-SP360M) was operated in 5.0 Pa of Ar (99.9995% purity). Films were deposited on SiO_2 glass substrate while applying a RF power of 100 W for 2.5 h. The as-deposited thin films were annealed in a temperature range between 700 and 1000 °C in air for 100 min. To attain the fixed annealing duration, the films were placed and then taken out from a box furnace at the certain temperatures.

Crystalline phases were characterized using X-ray diffraction (XRD) with monochromatized Cu Kα radiation (Rigaku, Ultima IV). Magnetic hysteresis was studied in a field of up to 1.5 T at room temperature using a vibrating sample magnetometer (Riken Denshi, BHV-50). The film thickness was estimated by observing their cross section in scanning electron microscopy (SEM) (JEOL, JSM-6390LV). The chemical compositions of the films were analyzed by fluorescent X-ray spectroscopy (XRF) (SII, SEA6000VX) in thin film FP mode. The microstructure of the annealed film was observed by using transmission electron microscope (TEM) (JEOL, JEM-2100F). The sample observed was a cross-sectional thin slice finished by Ar ion beam thinning.

3. Results and discussion

As-deposited films were amorphous independently on the film composition as shown in Fig. 1(a). Their film thickness was about 1, 0.9, 0.8 and 0.7 μm for $x = 0.25$, 0.33, 0.42 and 0.50, respectively, and decreased against the SiO_2 area ratio, x in the $(\alpha\text{-}Fe_2O_3)_{1-x}(SiO_2)_x$ composite target. Their Fe_2O_3/SiO_2 compositional ratio in the deposited films were also measured by using XRF to be 68/32, 60/40, 48/52 and 40/60 in at% for the films with $x = 0.25$, 0.33, 0.42 and 0.50, respectively. The film annealed at 900 °C was still amorphous at $x = 0.5$ (Fig. 1(b)). Fe_2O_3 appeared as metastable ε-phase at $x = 0.42$ and 0.33 (Figs. 1(c) and (d)) and then changed to α-phase at $x = 0.25$ (Fig. 1(e)). In higher SiO_2 content, Fe_2O_3 concentration was too thin to form its crystallite detectable in X-ray diffraction. The crystallite size grew with the increasing Fe_2O_3 content in the film to crystallize in ε- and α-Fe_2O_3. It was calculated to be 20, 25 and 40 nm by using Scherrer equation from a single diffraction peak observed at $2\theta \approx 33°$ for the thin films at

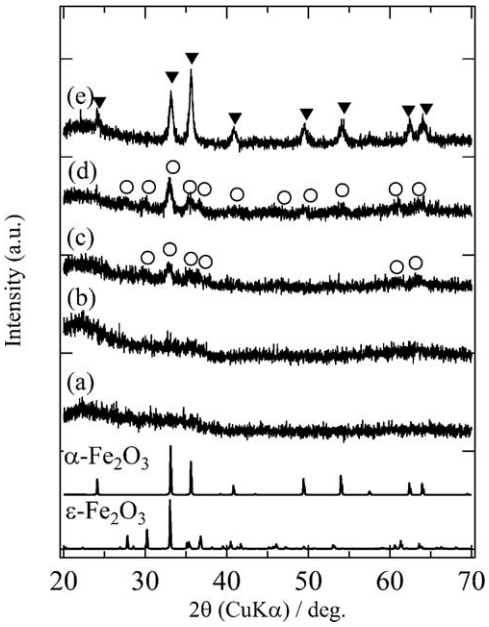

Fig. 1. XRD patterns for the as-deposited film at $x = 0.33$ (a) and annealed thin films at 900 °C for 100 min at (b) $x = 0.50$, (c) $x = 0.42$, (d) $x = 0.33$, and (e) $x = 0.25$ in $(Fe_2O_3)_{1-x}(SiO_2)_x$ targets. Symbols ○ and ▼ represent diffraction peaks for ε-Fe_2O_3 and α-Fe_2O_3, respectively. Theoretical patterns are also shown in the bottom using literature values for ε-Fe_2O_3[10] and α-Fe_2O_3.[21] The peak profile (peak positions and intensity ratio) of (c) and (d) corresponds to that of ε-Fe_2O_3.

$x = 0.42$, 0.33 and 0.25, respectively. The crystallite sizes for ε-phase were almost comparable to value obtained by sol–gel methods.[5,6,16]

TEM image of the annealed film at $x = 0.33$ shows dark grains of ca. 22 nm diameter in bright region as depicted in Fig. 2. The grain observed in TEM is almost similar to the crystallite size 25 nm of ε-Fe_2O_3 calculated from XRD (Fig. 1(d)). The dark grains and bright part might be ε-Fe_2O_3 and SiO_2 matrix, respectively. Composite of ε-Fe_2O_3 nanoparticle and amorphous SiO_2 matrix was successfully obtained by the simple thermal annealing of Fe–Si–O amorphous film.

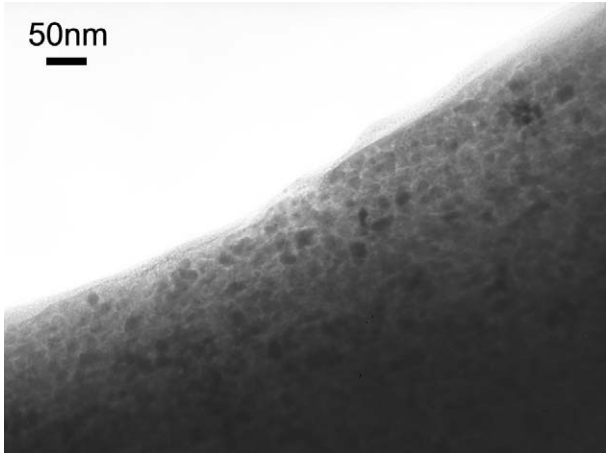

Fig. 2. TEM image of the film annealed at 900 °C for 100 min with $x = 0.33$ in $(\alpha\text{-}Fe_2O_3)_{1-x}(SiO_2)_x$ target.

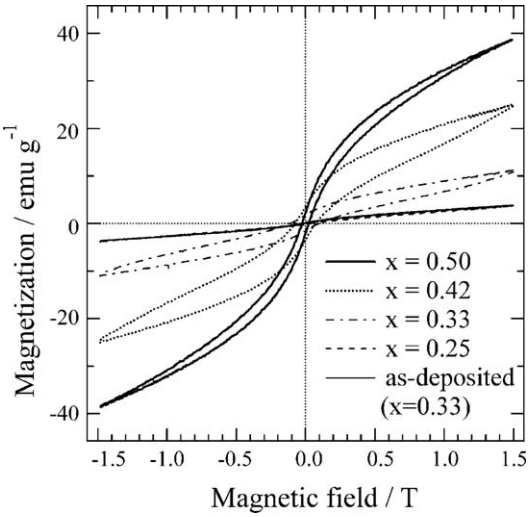

Fig. 3. Magnetic hysteresis of the as-deposited and annealed films. They were annealed at 900 °C for 100 min.

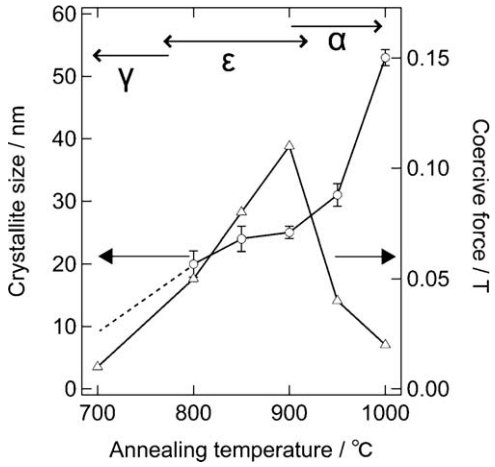

Fig. 4. Crystallite size and magnetic coercive force in the annealed films with $x = 0.33$ against its annealing temperature. Open circle and triangle represent crystallite size and coercive force, respectively. Dashed line shows expected changing in crystallite size below 800 °C because of a smaller size under detection limit in XRD. Upper arrows indicate observed crystalline Fe_2O_3 phases.

Fig. 3 shows the magnetization curves for the thin films as-deposited and annealed at 900 °C. Total Fe_2O_3 contents in each film were calculated by using film thickness and Fe_2O_3/SiO_2 compositional ratio in the films to show the magnetization per Fe_2O_3 weight in the figure. The as-deposited film was paramagnetic due to its amorphous structure. The annealed film at $x = 0.50$ showed magnetization curve having the highest magnetization, although it was again amorphous in XRD. The annealed films crystallized in ε-Fe_2O_3 exhibited a larger magnetic coercive force and lower magnetization than the values for $x = 0.50$. The largest coercive force of 0.10 T was obtained in the annealed film at $x = 0.33$. α-Fe_2O_3 observed at $x = 0.25$ showed a weak ferromagnetic hysteresis with very small coercive force due to its slightly canting in spins, i.e. Dzyaloshinsky–Moriya interaction.[2,3] The magnetization has been reported to be 80, 15 and 1 emu/g for γ-, ε- and α-Fe_2O_3, respectively.[5] γ-Fe_2O_3 has been reported to be stabilized in the smallest particle size among Fe_2O_3 phases.[16,17] The annealed film with $x = 0.50$ showed the highest magnetization probably because γ-Fe_2O_3 having a smaller crystallite size below detection limit in XRD crystallized in SiO_2 matrix forming nanocomposite. The crystal structures of the annealed films changed in the order of $\gamma \rightarrow \varepsilon \rightarrow \alpha$-$Fe_2O_3$ as the SiO_2 contents decrease with increasing in their crystallite size.

The size of Fe_2O_3 nanoparticles precipitated in SiO_2 matrix also changes with the annealing temperature. Fig. 4 depicts the annealing temperature dependence of the crystallite size obtained from the composite target of $x = 0.33$. ε-Fe_2O_3 with 20–25 nm in crystallite size was observed between 800 and 900 °C. Above 950 °C, the crystallite size steeply increased to over 50 nm at 1000 °C. As the crystallite size increased, crystal structure of the Fe_2O_3 changed to α-Fe_2O_3 reported to be stabilized above 30 nm in crystallite size. Their coercive force increased with increase in their crystallite size up to annealing temperature of 900 °C. The magnetic coercive force decreased with the phase transformation to α-Fe_2O_3. The crystallite size was successfully controlled by changing the annealing temperature, as well as changing the film composition. The present crystallite size around 25 nm suitable to obtain ε-Fe_2O_3 was comparable to the previously reported value in the preparation of ε-Fe_2O_3 in SiO_2 matrix[5,6,16] β-Fe_2O_3 did not precipitate even as an impurity phase in this study.

Magnetic coercivity values were summarized against crystallite size of Fe_2O_3 observed in any kinds among the present annealed films by changing either x-value or annealing temperature in Fig. 5. The smallest crystallite size observed in XRD was 20 nm for ε-Fe_2O_3. The annealed thin film with lesser iron content was XRD amorphous as in Fig. 1(b) and showed the largest magnetization in Fig. 3. Ferrimagnetic γ-Fe_2O_3 nanoparticles might precipitate in smaller size than 15 nm as X-ray amorphous as already suggested in phase transformation of Fe_2O_3 particle size.[16,17] Between 15 and 30 nm, we could obtain ε-Fe_2O_3/SiO_2 nanocomposite. In this region, the annealed film with crystallite size of 21 nm showed the highest coercive force of 0.14 T. α-Fe_2O_3 was observed above 30 nm crystallite size and it showed

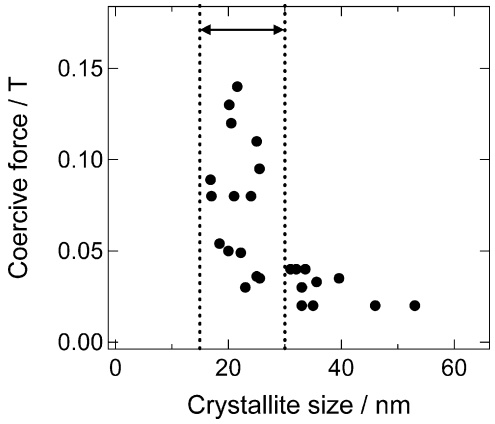

Fig. 5. Coercive force against the crystallite size in the annealed thin films. The ε- and α-Fe_2O_3 phases were observed in crystallite size between 15 nm and 30 nm and above, respectively. The film was X-ray amorphous in the size below 15 nm.

a small coercive force of around 0.01 T due to its weak ferromagnetism. The coercive force of 0.14 T in ε-Fe_2O_3/SiO_2 composite film observed in this study is much suppressed in contrast to the reported value of 2 T.[5–7] Small coercivity in ε-Fe_2O_3/SiO_2 nanocomposite was also reported by several groups.[8,9] The enormously large coercivity of ε-Fe_2O_3 was interpreted as mainly due to its large magnetocrystalline anisotropy ($K \sim 10^6$ erg/cm^3) and its appropriate particle size effect to suppress the movement of magnetic domain wall. It is well known that magnetic material has a maximal coercive force when its particle size is in critical size at which magnetic domain structure changes from single- to multi-domain.[22,23] It is difficult to obtain the ε-Fe_2O_3/SiO_2 nanocomposite thin film with very large coercivity in the present study because the discrepancy from the previous value is very large.

4. Conclusions

Fe_2O_3/SiO_2 nanocomposite thin film was obtained by annealing of the amorphous Fe–Si–O thin film deposited by RF-magnetron sputtering of $(\alpha\text{-}Fe_2O_3)_{1-x}/(SiO_2)_x$ composite targets by changing their area ratio, x. The crystal structure and crystallite size were controlled by changing thermal annealing condition and Fe_2O_3/SiO_2 compositional ratio. ε-Fe_2O_3 with crystallite size of 20–30 nm was obtained by annealing the film deposited using the target of SiO_2 area ratio, $x = 0.33$–0.42 at 900 °C. Lower SiO_2 area ratio and higher annealing temperature led to increase the crystallite size to more than 40 nm resulting in the formation of α-Fe_2O_3 phase showing a weak ferromagnetism. The annealed thin film was amorphous in the case of SiO_2 area ratio, $x > 0.50$. It showed the magnetic hysteresis having the largest magnetization and the smallest coercivity among the present study probably because of the γ-Fe_2O_3 precipitation in very small crystallite size. The ε-Fe_2O_3/SiO_2 nanocomposite thin film showed ferromagnetic hysteresis with the largest coercivity of 0.14 T at the maximum among the present products. Precipitation of the Fe_2O_3 in SiO_2 matrix from amorphous oxide thin film was successfully controlled by changing the annealing temperature and Fe_2O_3/SiO_2 compositional ratio.

References

1. Zboril R, Mashlan M, Petridis D. *Chem Mater* 2002;**14**:969–82.
2. Dzyaloshinsky I. *J Phys Chem Solids* 1958;**4**:241–55.
3. Moriya T. *Phys Rev* 1960;**120**:91–8.
4. Gilleo MA. *Phys Rev* 1958;**109**:777–81.
5. Jin J, Ohkoshi S, Hashimoto K. *Adv Mater* 2004;**16**:48–51.
6. Kurmoo M, Rehspringer JL, Hutlova A, D'Orleans C, Vilminot S, Estournes C, et al. *Chem Mater* 2005;**17**:1106–14.
7. Tseng YC, Souza-Neto NM, Haskel D, Gich M, Frontera C, Roig A, et al. *Phys Rev B* 2009;**79**:094404.
8. Brazda P, Niznansky D, Rehspringer JL, Vejparvova JP. *J Sol–Gel Sci Technol* 2009;**51**:78–83.
9. Nakamura T, Yamada Y, Yano K. *J Mater Chem* 2006;**16**:2417–9.
10. Tronc E, Chaneac C, Jolivet JP. *J Solid State Chem* 1998;**139**:93–104.
11. Ben-Der L, Fischbein E, Kalman Z. *Acta Cryst B* 1976;**32**:667.
12. Svendsen MB. *Naturwissenschaften* 1958;**45**:542.
13. Ikeda Y, Takano M, Bando Y. *Bull Inst Chem Res Kyoto Univ* 1986;**64**:249–58.
14. Chaneac C, Tronc E, Jolivet JP. *Nanostruct Mater* 1995;**6**:715–8.
15. Chaneac C, Tronc E, Jolivet JP. *J Mater Chem* 1996;**6**:1905–11.
16. Gich M, Roig A, Taboada E, Molins E, Bonafos C, Snoeck E. *Faraday Discuss* 2007;**136**:345–54.
17. Sakurai S, Namai A, Hashimoto K, Ohkoshi S. *J Am Chem Soc* 2009;**131**:18299–303.
18. Long J, Laughlin DE, McHenry ME. *J Appl Phys* 2008;**103**:07E708.
19. Trudeau ML. *Mater Sci Eng A* 1995;**204**:233–9.
20. Rivero G, Multigner M, Garcia JM, Crespo P, Hernando A. *J Magn Magn Mater* 1998;**177–181**:119–20.
21. Blake RL, Hessevick RE, Zoltai T, Finger LW. *Am Mineral* 1966;**51**:123–9.
22. Kittel C. *Phys Rev* 1946;**70**:965–71.
23. Kneller EF, Luborsky FE. *J Appl Phys* 1963;**34**:656–8.